J Fluoresc (2011) 21:1285–1292
DOI 10.1007/s10895-010-0811-1

ORIGINAL PAPER

Quantitative Analysis of Intracellular Calcium and Mitochondrial Kinetic Fluorescence Changes in GSNO-induced Thymocyte Early Apoptosis

Xiaochen Liu · Danying Lin · Wanyun Ma

Received: 28 April 2010 / Accepted: 29 December 2010 / Published online: 6 January 2011

Abstract A fluorescence microscopy imaging technique was applied to observe the single-cell kinetic changes of intracellular Ca^{2+} concentration ($[Ca^{2+}]_i$) and mitochondrial membrane potential ($\Delta\Psi_m$) during the early stage of S-nitrosoglutathione (GSNO)-induced thymocytes apoptosis. The kinetic features of $[Ca^{2+}]_i$ and $\Delta\Psi_m$ were quantitatively analyzed and compared by fitting the fluorescence intensity data. The mathematical parameter, inflection point which indicated the time point when $[Ca^{2+}]_i$ or $\Delta\Psi_m$ changed the most rapidly, was proposed to analyze the fitting curve. The results revealed that the inflection point of $[Ca^{2+}]_i$ always appeared prior to that of $\Delta\Psi_m$ during apoptosis induced by a certain GSNO concentration. Both the $[Ca^{2+}]_i$ and $\Delta\Psi_m$ changed in a GSNO concentration-dependent manner. Another parameter, half-max effect point was also employed and displayed the similar results. Such quantitative analyses of real-time observations at the single-cell level are useful for interpreting the sequence of the biological events operating in GSNO-induced thymocyte apoptosis.

Keywords Intracellular Ca^{2+} concentration ($[Ca^{2+}]_i$) · Mitochondria · Inflection point · Real-time fluorescence imaging · Apoptosis

X. Liu · D. Lin · W. Ma (✉)
Key Laboratory for Atomic and Molecular Nanosciences of Education Ministry, Department of Physics, Tsinghua University, Beijing 100084, China
e-mail: mawy@mail.tsinghua.edu.cn

D. Lin
Institute of Optoelectronics, Shenzhen University, Shenzhen 518060, China

Introduction

Apoptosis, or programmed cell death, is of vital importance for normal tissue development and homeostasis of the immune system and involves a series of biochemical events [1–5]. On one hand, cytoplasmic Ca^{2+} plays an important role in many cellular and subcellular activities as a universal second messenger. Its changes are related to numerous functions of the cells [6]. Ca^{2+} signaling has been focused upon in a number of apoptosis studies, and it is even regarded as the first intracellular signaling event and occurs upstream of cytochrome C release [3, 7, 8]. On the other hand, the mitochondrial pathway is one of the pathways for apoptosis, and is the main mechanism in animal cells. Mitochondrial membrane potential ($\Delta\Psi_m$) is associated with the intracellular calcium concentration ($[Ca^{2+}]_i$) during this process, especially in the early stage [3]. As intracellular calcium stores, mitochondria are able to accumulate calcium. However, excessive Ca^{2+} load to the mitochondria may induce apoptosis by stimulating the release of apoptosis promoting factors [3, 9–12]. Most studies only focus the attention on record of the kinetic fluorescence variations, which results in a lack of a further quantitative analysis.

Quantitative fluorescence measurements have been used in biological research areas, such as protein-protein interactions [13], the time-resolved fluorescence spectrum of the cortical sarcoma and adjacent normal tissue [14] and so on [4, 15, 16]. In addition, mathematical parameters of the kinetic curves provide more information and help us to understand the biological events better. For instance, the inflection points are used to research the onset of puberty in sheep and measure the onion cultivars with image analysis [17, 18]. Dissociation constants are calculated to measure

the binding affinities of interacting protein pairs [13]. Decay constants are employed to quantify the differences between the normal and tumor tissues [14].

S-nitrosoglutathione (GSNO) is the S-nitroso derivative of glutathione. It can induce thymocyte apoptosis effectively at low concentrations [19]. The initiating time point of the apoptosis is mostly around 2 h [19, 20]. In the present study, we proposed to assess the dynamic features of the two apoptotic events, $[Ca^{2+}]_i$ and $\Delta\Psi_m$, at the single-cell level, coupled with a mathematical parameter: inflection point. The real-time changes in $[Ca^{2+}]_i$ and $\Delta\Psi_m$ in single thymocyte were investigated using a fast fluorescence microscopy imaging technique [20]. The results from quantitative analysis revealed valuable information about the intracellular variations in $[Ca^{2+}]_i$ and $\Delta\Psi_m$ after GSNO stimulation. We found that the inflection points for $[Ca^{2+}]_i$ curves always appeared prior to that for $\Delta\Psi_m$ using the same concentration of GSNO for stimulation. Additionally, these parameters revealed a GSNO concentration-dependent property.

Material and Methods

Reagents

DCCM-2 medium was purchased from Biological Industries (Israel). Glutathione was bought from Sigma Chemical (USA). Fluorescent indicators Fluo-3/AM and Rhodamine 123 (Rh123) were purchased from Invitrogen (USA) and KeyGen Biotech.Co. (Nanjing, China) respectively. Ficoll lymphocyte separated medium (with specific gravity of 1.092) was obtained from Hengxin Chemical Reagent (Shanghai, China). Phosphate buffered saline (PBS) and D-Hank's buffer (without $CaCl_2$, $MgSO_4$ and phenolsulfonphthalein) were both acquired from Biosea Biotechnology (Beijing, China).

GSNO Synthesis

GSNO, the reductive S-nitroso derivative of glutathione, must be freshly synthesized prior to the experiments according to the literature [20]. The mixture was protected from light during the whole procedure.

Preparation of Thymocytes

Inbred BALB/C mice were purchased from the Experimental Animal Center of Institute of Genetics and Developmental Biology, Academia Sinica (Beijing, China). Three-week-old mice, with the mean weight of 12.5±0.9 g, were sacrificed by cervical dislocation. The thymocytes were obtained by gently and repeatedly pressing the thymus against a piece of nylon net submerged in D-Hank's buffer. Single cells were resuspended to 1×10^7 cells/ml in DCCM-2 medium, divided into small parts for use. Three separate experiments were performed.

Loading of Fluorescent Indicators and Sample Grouping

Fluo-3 was used as the Ca^{2+} indicator and cells were loaded with its ester form, Fluo-3/AM. Rh123 was used as the mitochondrial indicator. Thymocytes were washed twice with D-Hank's buffer and reacted with Fluo-3/AM (final concentration, 4.4 μM) for 20 min or Rh123 (final concentration, 26 μM) for 10 min. The labeling solution was exchanged for a dye-free solution after the incubation. Each cell suspension was transferred into a MatTek glass-bottomed culture dish and allowed to rest for 20 min. Each suspension was then continuously imaged for 180 s to obtain the initial fluorescence intensity before treatment with different concentrations of GSNO as the trigger. A total of six experimental groups were set up: (1) $Control_{Ca}$; (2) $GSNO\text{-}I_{Ca}$; (3) $GSNO\text{-}II_{Ca}$; (4) $Control_{mito}$; (5) $GSNO\text{-}I_{mito}$; and (6) $GSNO\text{-}II_{mito}$. GSNO-I and GSNO-II denoted treatments with 0.3 and 0.6 mM GSNO, respectively, while Control referred medium without GSNO. The subscript "Ca" referred to Fluo-3 labeling while "mito" referred to Rh123 labeling. After addition of each trigger concentration to the medium, the real-time fluorescence imaging was continued for 540 s. The exposure time was 200 ms with an interval of 5 s. Transmission images of thymocytes were obtained to show the shapes and sites of the cells.

Fluorescence Microscopic Imaging Setup

Fluorescence imaging was carried out on an intensified charge-coupled device (ICCD)-based real-time fluorescence microscopy system [20], which was composed mainly of a TE2000 inverted microscope (Nikon, Japan) with a Nikon 100× *N.A.* 1.3 oil objective, an I-PentaMAX Gen IV ICCD camera (Roper Scientific, USA), and an xenon arc lamp in the Lambda DG-4 Wavelength Switcher (Sutter Instrument, USA). Selective excitation was produced through a 484± 7.5 nm band-pass filter, and emitted fluorescence was collected through a 535±20 nm one. Real-time fluorescence was monitored and quantitatively analyzed with the MetaMorph software (Universal Imaging Co., USA). Excitation light was adequately attenuated. Photobleaching and cell damage were minimized by auto-synchronizing the exciting shutter and the exposure shutter, i.e. cells were exposed to light only during exposure but not at the interval. This ICCD fluorescence micro-imaging system possessed the advantages of high-performance thermoelectric cooling function to reduce noise, and a gain high enough to detect extremely low light [20].

Processing of the Fluo-3 Fluorescence Data

The Fluo-3 fluorescence intensity of each cell was obtained by subtracting the image background. A pseudo-ratio, $(\Delta F/F_0) = (F - F_0)/F_0$, was introduced. F_0 was the Fluo-3 fluorescence intensity of the cell before stimulation and F indicated the measured fluorescence intensity. $(\Delta F/F_0)$ is proportional to $\Delta[Ca^{2+}]_i$, and was reported to reflect the variation in $[Ca^{2+}]_i$ [6]. $[Ca^{2+}]_i$ increased rapidly after the GSNO treatments and reached a plateau, $(\Delta F/F_0)_f$. Therefore, the Origin software (OriginLab Co., USA) was used to fit a curve to the $(\Delta F/F_0)$ data points, with the fitting formula:

$$y = y_c + \frac{y - y_c}{1 + (t/t_0)^p}, \quad (1)$$

where y_c indicated the plateau $(\Delta F/F_0)_f$. Correlation coefficients were all greater than 0.9. t_0 and p are simply fitting parameters. The inflection point also known as inflexion point of the fitted curve was given by:

$$T = t_0 \left(\frac{p-1}{p+1}\right)^{1/p}, \quad (2)$$

At the inflection point T, the second derivative $(d^2y/dt^2)=0$ and the slope of the curve (dy/dt) is the maximum. T is the time point when y changes the maximum. In this case, T_{Ca} indicated the time point when $[Ca^{2+}]_i$ changed the most rapidly.

Processing of the Rh123 Fluorescence Data

Rh123 is readily sequestered by active mitochondria owing to the membrane potential $\Delta\Psi_m$. When $\Delta\Psi_m$ depolarizes, Rh123 is released into the cytosol. Therefore, loss of $\Delta\Psi_m$ in single cells can be estimated by measuring the decrease in Rh123 fluorescence [12, 21–24]. Although the Rh123 fluorescence intensity in each cell hardly varied during the whole observation period, the distribution of the fluorescent regions clearly changed. Taking the mean fluorescence intensity of each cell during the whole observation period as a threshold, we considered that the regions in which the fluorescence intensity was above the threshold were mitochondrial areas, and that the other regions were cytoplasmic areas. The mean fluorescence intensity in the mitochondrial areas was designated F_m, while that in the cytoplasmic areas was designated F_c. Since the F_c value in the GSNO-treated cells increased rapidly and reached a plateau $(F_c)_f$, similar to the case for $[Ca^{2+}]_i$, the fitting formula (1) was also used to fit a curve to the F_c data points, and y_c indicated $(F_c)_f$ in this case. Correlation coefficients were all also greater than 0.9. t_0 and p were simply fitting parameters. The inflection point of the fitted curve with formula (2), designated T_{mito}, indicated the time point when Rh123 diffused the most rapidly, and reflected the time point at which $\Delta\Psi_m$ changed the most rapidly.

Comparison with a Conventional Parameter Half-Maximal Effect $t_{1/2}$

The conventional parameter $t_{1/2}$, which is usually used as the time point when half-maximal effects are observed, was also calculated for comparisons with T_{Ca} and T_{mito}. The time point of half-maximal $(\Delta F/F_0)$ in the GSNO-I_{Ca} and GSNO-II_{Ca} groups were designated $t_{1/2Ca}$ and the time point of half-maximal F_c in the GSNO-I_{mito} and GSNO-II_{mito} groups were designated $t_{1/2mito}$. The $t_{1/2}$ were used to indicate the sequence of events during apoptosis in a previous study [7].

Statistical Analysis

Data were analyzed for statistically significant differences using a paired Student's *t*-test. The compiled data were expressed as the mean ± SEM, with n denoting the number of thymocytes studied.

Results

Kinetic Changes in $[Ca^{2+}]_i$ during GSNO-Induced Early Apoptosis in Thymocytes

Figure 1 shows the transmission and fluorescence images of $Control_{Ca}$ (Fig. 1(a)), GSNO-I_{Ca} (Fig. 1(b)) and GSNO-II_{Ca} (Fig. 1(c)) groups. Fluorescence changes were not found in Fig. 1(a) middle and right images, whereas after GSNO induced, the fluorescence in thymocytes had evidently increased (Fig. 1(b) (c) right column).

Figure 2 shows typical kinetic curves of $(\Delta F/F_0)$ in single cells from the $Control_{Ca}$, GSNO-I_{Ca} and GSNO-II_{Ca} groups. As mentioned above, $\Delta F/F_0$ is proportional to $\Delta[Ca^{2+}]_i$, and reflects the changes in $[Ca^{2+}]_i$. The curves for the GSNO-I_{Ca} and GSNO-II_{Ca} groups revealed that the $[Ca^{2+}]_i$ in each single cell began to increase rapidly after GSNO addition (dashed lines) and finally reached a plateau $(\Delta F/F_0)_f$. The plateau values showed a concentration-dependency. Specifically, the plateau value for $[Ca^{2+}]_i$ in the GSNO-I_{Ca} group treated with 0.3 mM GSNO was smaller than that in the GSNO-II_{Ca} group treated with 0.6 mM GSNO.

An example of a fitted curve using formula (1) is also shown in Fig. 1 for the data points of a cell in the GSNO-II_{Ca} group (black line). In this study, the inflection point T_{Ca} of the fitted curve was extracted with formula (2) and used to represent the time point when the $[Ca^{2+}]_i$ changed

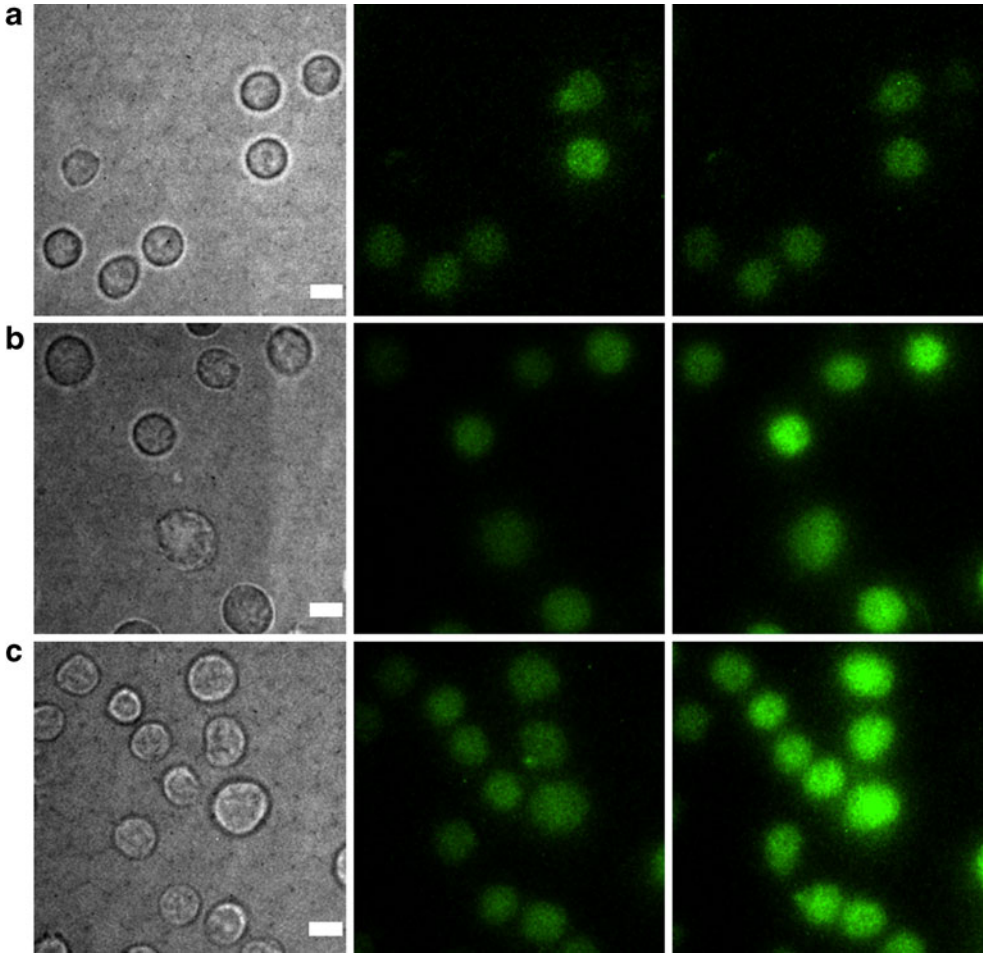

Fig. 1 Transmission images (left) and fluorescence images before any treated (middle) as well as fluorescence images after treated (right) of **a** $Control_{Ca}$, **b** GSNO-I_{Ca} and **c** GSNO-II_{Ca} groups.Grouping: $Control_{Ca}$ - treated with 100 μl D-Hank's; GSNO-I_{Ca} - treated with 0.3 mM GSNO; GSNO-II_{Ca} - treated with 0.6 mM GSNO. Scale bar: 5 μm

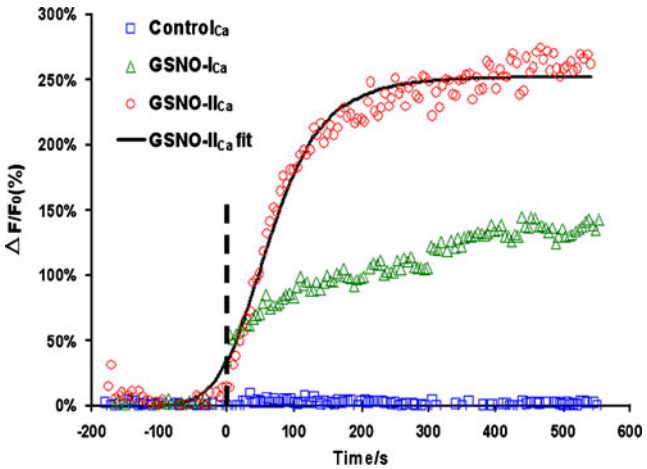

Fig. 2 Typical $\Delta F/F_0$ kinetic curves in single cells from the $Control_{Ca}$, GSNO-I_{Ca} and GSNO-II_{Ca} groups. $\Delta F=F-F_0$, F was the fluorescence intensity of the cell at time *t*, F_0 was the fluorescence intensity of the cell before time $t=0$ (when GSNO stimulation begins, shown as a dash line). Grouping: $Control_{Ca}$ - treated with 100 μl D-Hank's at $t=0$; GSNO-I_{Ca} - treated with 0.3 mM GSNO at $t=0$; GSNO-II_{Ca} - treated with 0.6 mM GSNO at $t=0$. Black line: fitting curve for data of the cell in group GSNO-II_{Ca} using formula (1)

the most rapidly. This point is an important kinetic parameter of the $[Ca^{2+}]_i$ changes in single cells. Statistical data will be provided later during comparisons with the other results.

Kinetic Changes in $\Delta\Psi_m$ during GSNO-Induced Early Apoptosis in Thymocytes

Figures 3 and 4 show that the mitochondria in the thymocytes were labeled with Rh123. Little fluorescence was observed in other areas of the cells before treatment with GSNO (Fig. 3 middle column and $t<0$ in Fig. 4). After GSNO treatment, the fluorescence intensity in the mitochondrial regions decreased rapidly, while that in the remaining areas increased gradually (Fig.3(b) (c) right column and $t>0$ in Fig. 4). After calculating the fluorescence intensity in each single cell, we were surprised to find that it remained almost unchanged during the whole observation period (720 s). This result indicated that Rh123 was released from the mitochondria into the cytoplasm owing to loss of $\Delta\Psi_m$ during GSNO treatment, but the cell membrane remained intact and maintained the fluorescent indicators inside the cell in the early stage of apoptosis.

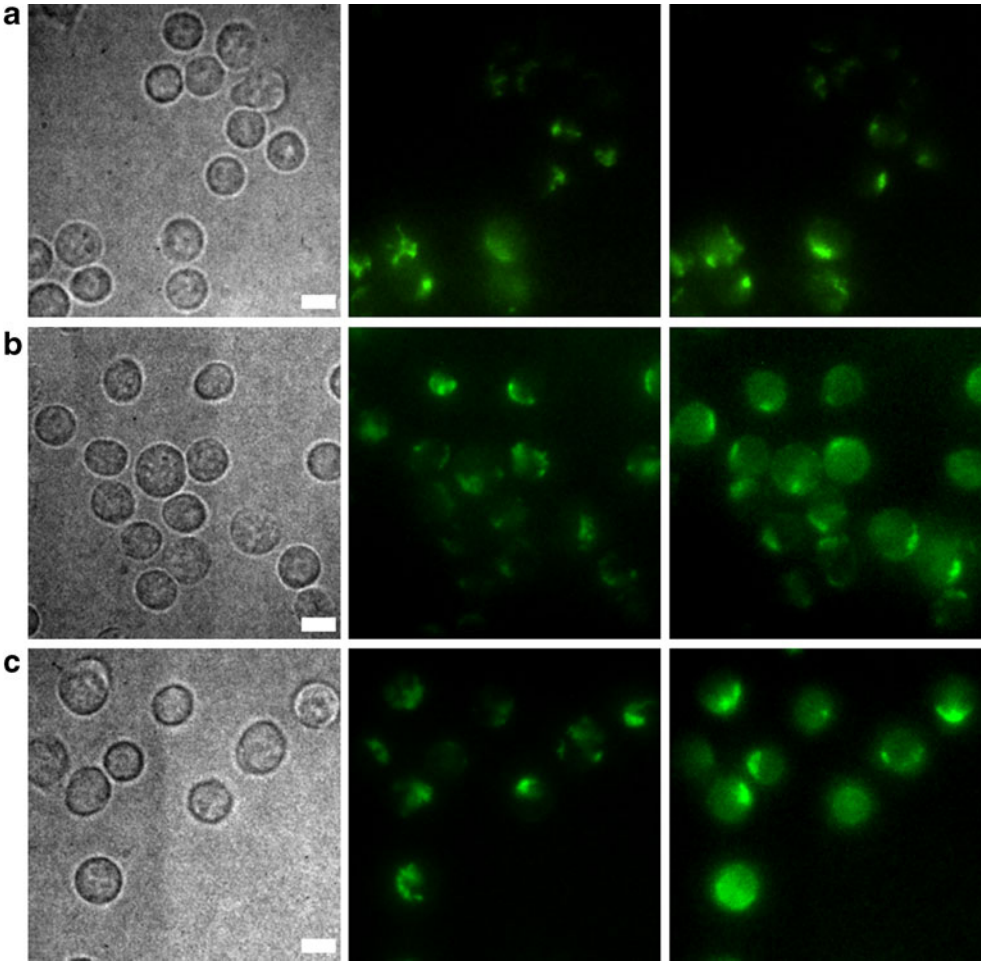

Fig. 3 Transmission images (*left*) and fluorescence images before any treated (*middle*) as well as fluorescence images after treated (*right*) of **a** $Control_{mito}$, **b** $GSNO\text{-}I_{mito}$ and **c** $GSNO\text{-}II_{mito}$ groups. Grouping: $Control_{mito}$ - treated with 100 μl D-Hank's; $GSNO\text{-}I_{mito}$ - treated with 0.3 mM GSNO; $GSNO\text{-}II_{mito}$ - treated with 0.6 mM GSNO. Scale bar: 5 μm

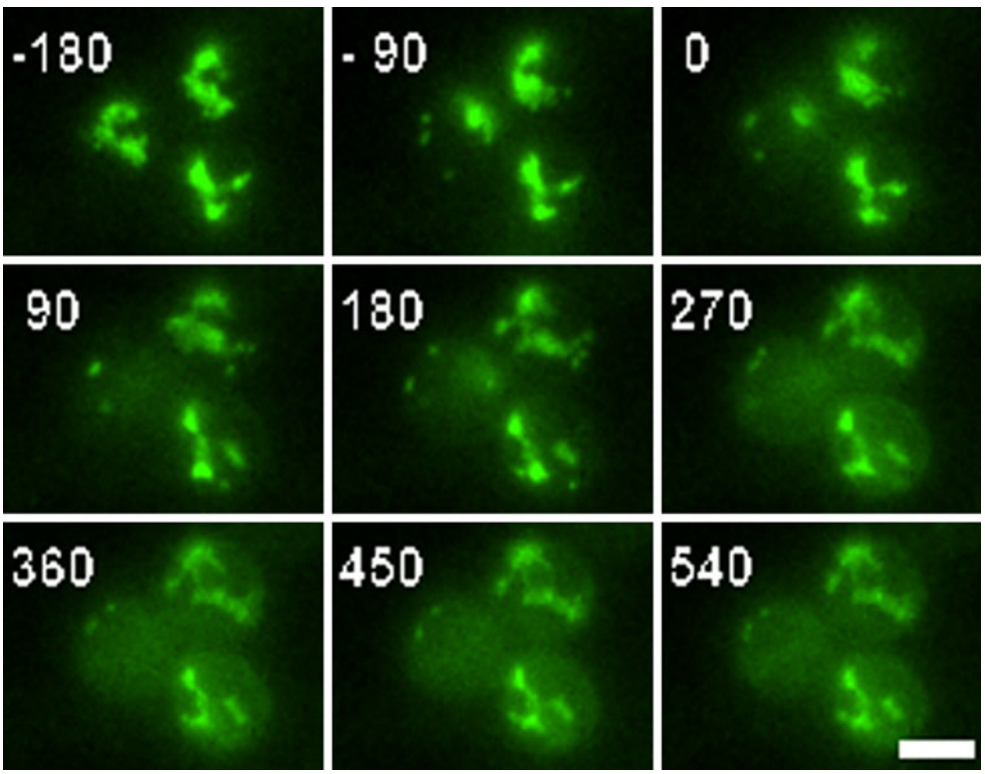

Fig. 4 Time-lapse images of mitochondrial morphological changes in group $GSNO\text{-}II_{mito}$. Green pseudo color stood for the Rh123 fluorescence. The number in each image (units: s) corresponded to its image time relative to the time point of GSNO (0.6 mM) addition. Scale bar: 5 μm

Typical kinetic curves of F_c and F_m in single cells from the GSNO-II_{mito} group are shown in Fig. 5. These curves were similar to those in the GSNO-I_{mito} group. As described in Materials and Methods, F_m indicated the fluorescence intensity in the mitochondrial areas and F_c indicated the fluorescence intensity in the cytoplasmic areas. The F_m values in a cell from the $Control_{mito}$ group (blue squares) did not show any obvious changes during the observation period. However, the fluorescence intensity in mitochondrial areas (F_m, red rings) in a cell from the GSNO-II_{mito} group decreased immediately after treatment with 0.6 mM GSNO, while the fluorescence intensity in the cytoplasmic areas (F_c, green triangles) increased simultaneously. The kinetic process of mitochondrial damage, as well as the loss of $\Delta\Psi_m$, was recorded in real time via the release of Rh123 from mitochondria into the cytoplasm with such curves. The plateau $(F_c)_f$ was smaller in the GSNO-I_{mito} group than in the GSNO-II_{mito} group (data not shown), similar to the relationship between the final values of $[Ca^{2+}]_i$ in the GSNO-I_{Ca} and GSNO-II_{Ca} groups. These results indicated that the lower concentration of GSNO caused less variation in $\Delta\Psi_m$.

Fitting using formula (1) was carried out for the data points of F_c in the cells of the GSNO-I_{mito} and GSNO-II_{mito} groups. The inflection point T_{mito} of the fitted curve was used to represent the time point when the fluorescence intensity in the cytoplasmic areas changed the most rapidly, and it also reflected the time point when $\Delta\Psi_m$ collapsed the most rapidly. Statistical data will be provided in the following paragraphs during comparisons with the other results.

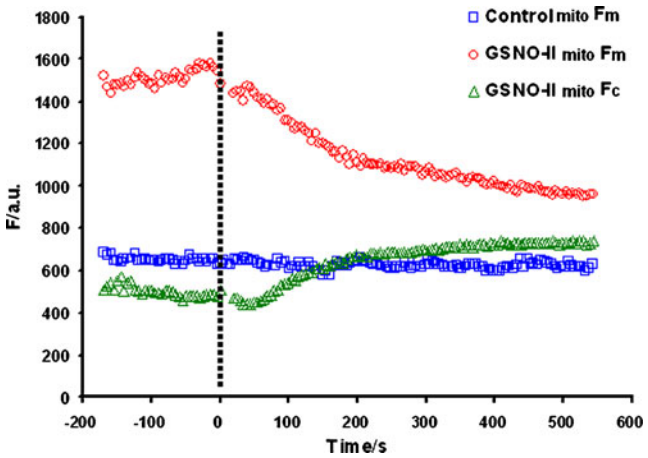

Fig. 5 Typical kinetic curves of fluorescence intensity F_m in active mitochondrial regions and fluorescence intensity F_c in the cytoplasm. A dash line indicated time point t=0, when GSNO stimulation began. Grouping: $Control_{mito}$ F_m - kinetic curve of F_m in cells treated with 100 μl D-Hank's at t=0; GSNO-II_{mito} F_m - kinetic curve of F_m in cells treated with 0.6 mM GSNO at t=0; GSNO-II_{mito} F_c - kinetic curve of F_c in cells treated with 0.6 mM GSNO at t=0

Statistical Data and Comparisons Between the Changes in $[Ca^{2+}]_i$ and $\Delta\Psi_m$

Figure 6 shows the statistical data for the T values in all the GSNO-treated groups, *i.e.* T_{Ca} (n=30 cells) in the GSNO-I_{Ca} and GSNO-II_{Ca} groups and T_{mito} (n=25 cells) in the GSNO-I_{mito} and GSNO-II_{mito} groups. The mean T_{Ca} values in the GSNO-I_{Ca} and GSNO-II_{Ca} groups were 148±22 and 48±3 s, respectively. In other words, the mean T_{Ca} in the GSNO-I_{Ca} group was distinctly bigger than that in the GSNO-II_{Ca} group. The lower concentration of GSNO caused a posterior appearance of T_{Ca} and a slower change in $[Ca^{2+}]_i$, revealing clear concentration-dependency. However, the mean T_{mito} in the GSNO-I_{mito} group was only slightly bigger than that in the GSNO-II_{mito} group (169±20 and 151±11 s, respectively). The variations in T_{mito} and $\Delta\Psi_m$ did not display obvious concentration-dependency.

Considering the situations when the same GSNO concentration was used, a comparison of T_{Ca} with T_{mito} was carried out. In the GSNO-I_{Ca} and GSNO-I_{mito} groups treated with 0.3 mM GSNO, the mean T_{Ca} seemed smaller than the mean T_{mito} (148±22 s vs. 169±20 s). Furthermore, when 0.6 mM GSNO was used (groups GSNO-II_{Ca} and GSNO-II_{mito}), the mean T_{Ca} was also smaller than the mean T_{mito} (48±3 s vs. 151±11 s). The inflection points indicated the time point when the $[Ca^{2+}]_i$ or $\Delta\Psi_m$ changed the most rapidly. Hence, these results revealed that the time point of $[Ca^{2+}]_i$ changed the fastest always appeared prior to that of

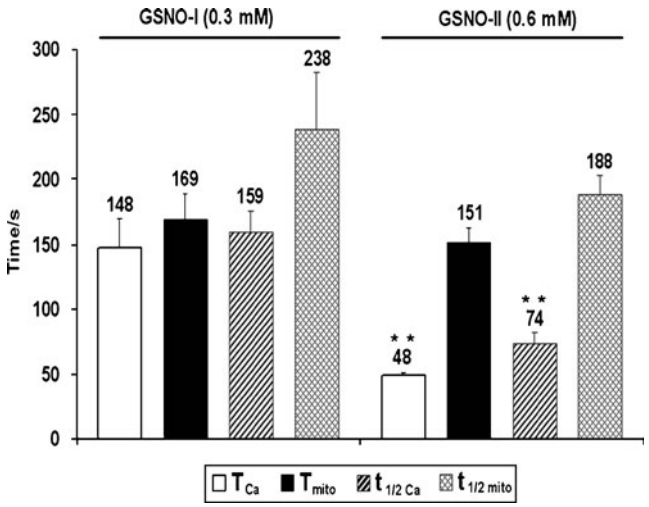

Fig. 6 Statistical results of kinetic parameters T and $t_{1/2}$ extracted from fitting curves. T_{Ca}: the time point when $[Ca^{2+}]_i$ changed the most rapidly; T_{mito}: the time point when $\Delta\Psi_m$ changed the most rapidly; $t_{1/2Ca}$: the time point when half-maximal effects of $\Delta F/F_0$ were observed in the GSNO-I_{Ca} and GSNO-II_{Ca} groups; $t_{1/2mito}$: the time point when half-maximal effects of F_c were observed in the GSNO-I_{mito} and GSNO-II_{mito} groups. Statistical results were expressed as mean ± SEM (for groups GSNO-I_{Ca} and GSNO-II_{Ca}, n=30; for groups GSNO-I_{mito} and GSNO-II_{mito}, n=25). * * P<0.01 vs. GSNO-I group

$\Delta\Psi_m$, regardless of the GSNO concentration used for the induction.

The parameter $t_{1/2}$, denoting the time point when half-maximal effects were observed, was also calculated for comparisons with T_{Ca} and T_{mito}. On one hand, the $t_{1/2}$ value was always larger than the T value in each group, regardless of the cellular events ($[Ca^{2+}]_i$ or $\Delta\Psi_m$) examined or the concentration of GSNO used, which can be seen in Fig. 6. On other hand, the relationships between $t_{1/2Ca}$ and $t_{1/2mito}$ were consistent with the above-described relationships between T_{Ca} and T_{mito}. In brief, both $t_{1/2Ca}$ and $t_{1/2mito}$ were dependent on the GSNO concentration. Besides, $t_{1/2Ca}$ was always smaller than $t_{1/2mito}$ under a certain GSNO-induced concentration.

Discussion and Conclusion

In the present study, several factors were taken into consideration to guarantee the accuracy of the fluorescence data for quantitative analysis. First, the imaging system minimized the phototoxicity toward living cells and photobleaching of the fluorescent dyes by auto-synchronizing the excitation shutter with the exposure shutter, as described in Materials and Methods. This technique minimized the exposure time of the cells to light to the maximum extent. Second, the ICCD-based fluorescence microscopy imaging system was equipped with a highly sensitive and efficient detector in order to capture the exact moments when the signals began to change or changed the most rapidly. Third, subtraction of the image background was carried out before any data processing. As such, the validity and reliability of the present study were guaranteed.

Kinetic analyses of a series of biochemical and cellular events during thapsigargin-induced thymocyte apoptosis have been reported [7]. In that study, it was shown that the time required to observe half-maximal effects ($t_{1/2}$) was used to determine the sequence of events occurring during the execution of the mitochondria-dependent cell death program. The first intracellular signal observed after thapsigargin addition was an increase in cytosolic $[Ca^{2+}]_i$ within a few minutes, followed by mitochondrial depolarization, cytochrome C release and DNA laddering in that order [7]. The inflection points represent important feature of the curves [17, 18, 25]. In the present study, two cellular events, changes of $[Ca^{2+}]_i$ and $\Delta\Psi_m$ were observed during the apoptotic process at the single-cell level, and a curve fitting method with the characteristic parameter T (inflection point of the fitted curve) was utilized to study the two kinetic events. Inflection point T denoted the time when curve value changed the maximum, whereas $t_{1/2}$ was the time point corresponding to the half-maximal effect of the curve. As the results show that the T values offered information that differed from, but was consistent with, the parameter $t_{1/2}$ employed in Bustamante's study. Briefly, T_{Ca} appeared prior to T_{mito} under a certain GSNO-induced concentration, as well as $t_{1/2Ca}$ and $t_{1/2mito}$. Our results suggest that T values can be used not only to establish the sequence of events during apoptosis, but to detect the most active moments that are important for nonlinear reactions.

GSNO has been reported to play a dual role of inducing thymocyte apoptosis at low concentrations and inhibiting thymocyte apoptosis at high concentrations [19]. The concentrations of 0.3 and 0.6 mM used in our experiments were both effective concentrations for inducing thymocyte apoptosis, as reported previously [19]. On this premise, our experiments suggested that cytosolic $[Ca^{2+}]_i$ increased rapidly and reached a plateau during GSNO-induced early apoptosis, while $\Delta\Psi_m$ declined simultaneously. Meanwhile, the time point when $\Delta\Psi_m$ changed the most rapidly, T_{mito}, always appeared after T_{Ca} when the same concentration of GSNO was used for stimulation. This consequence appeared more obviously from 0.6 mM GSNO calculated data than that from 0.3 mM GSNO group. The possible explanation for the results might be that the varieties in 0.3 mM were smaller and not evident as that in 0.6 mM. Comparisons between the different concentration groups revealed that the variation ranges of both $[Ca^{2+}]_i$ and $\Delta\Psi_m$ became broader with the higher concentration of GSNO and that T_{Ca} was smaller. These results demonstrate that a correlation exists between $[Ca^{2+}]_i$ and the concentration of GSNO. It has been proposed that $[Ca^{2+}]_i$ participate in early apoptosis by regulating apoptosis through mitochondrial calcium overload [3, 10]. As one type of intracellular calcium store, mitochondria are able to accumulate calcium. However, long-lasting global $[Ca^{2+}]_i$ increases may result in the accumulation of vast amounts of Ca^{2+} in the mitochondria, thereby causing damage to the mitochondria and leading to the induction of apoptosis. Our present experiment results, especially the relationships between T_{Ca} and T_{mito}, seem to support this apoptosis model based on mitochondrial calcium overload after GSNO induction.

In summary, using an ICCD-based real-time fluorescence microscopy imaging technique, we have studied the kinetic changes in $[Ca^{2+}]_i$ and $\Delta\Psi_m$ in GSNO-induced early apoptosis of thymocytes. By fitting the experimental data and calculating the parameters inflection point as well as half-max effect point, the kinetic features of $[Ca^{2+}]_i$ and $\Delta\Psi_m$ were quantitatively analyzed. On one hand, the time point for rapidest $[Ca^{2+}]_i$ change always appeared prior to that for $\Delta\Psi_m$ using the same concentration of GSNO for stimulation, revealing the correlation between the two apoptotic events. On the other hand, when a higher concentration of GSNO was used for apoptosis induction, the $[Ca^{2+}]_i$ increased and the $\Delta\Psi_m$ declined in a concentration-dependent manner. Thus, we believe that

mathematical model and quantitative analysis are a powerful tool for interpretating the cellular events. Inflection point, a valid mathematical parameter of the kinetic curves, can facilitate our understanding of the biological events.

Acknowledgements This work was supported by the National Nature Science Foundation of China (No. 90919012 and No. 10874099), Tsinghua University Initiative Scientific Research Program (2010THZ01) and the Doctoral Program Research Fund of Chinese Ministry of Education (Grant 20090002110065). We thank Professor Shaojin Duan for helpful discussion.

References

1. Susan E (2007) Apoptosis: a review of programmed cell death. Toxicol Pathol 35:495–516
2. Chang MK, Binder CJ, Miller YI, Subbanagounder G, Silverman GJ, Berliner JA, Witztum JL (2004) Apoptotic cells with oxidation-specific epitopes are immunogenic and proinflammatory. J Exp Med 200:1359–1370
3. Smaili SS, Hsu YT, Carvalho ACP, Rosenstock TR, Sharpe JC, Youle RJ (2003) Mitochondria, calcium and pro-apoptotic proteins as mediators in cell death signaling. Braz J Med Biol Res 36:183–190
4. Duan SJ, Wan L, Fu WJ, Pan H, Ding Q, Chen C, Han P, Zhu X, Du L, Liu H, Chen Y, Yan X, Deng M, Qian M (2009) Nonlinear cooperation of p53-ING1-induced bax expression and protein S-nitrosylation in GSNO-induced thymocyte apoptosis: a quantitative approach with cross-platform validation. Apoptosis 14:236–245
5. Malcomson RDG, Oram SH, Harrison DJ (1996) The importance of apoptosis: is it real or imaginary? Biologicals 24:295–299
6. Takahashi A, Camacho P, Lechleiter JD, Herman B (1999) Measurement of intracellular calcium. Physiol Rev 79:1089–1125
7. Bustamante J, Di Libero E, Fernandez-Cobo M, Monti N, Cadenas E, Boveris A (2004) Kinetic analysis of thapsigargin-induced thymocyte apoptosis. Free Radic Bio Med 37:1490–1498
8. Pu Y, Luo KQ, Chang DC (2002) A Ca^{2+} signal is found upstream of cytochrome c release during apoptosis in Hela cell. Biochem Biophys Res Co 299:762–769
9. Roy SS, Hajnóczky G (2008) Calcium, mitochondria and apoptosis studied by fluorescence measurements. Methods 46:213–223
10. Guo J, Pu YM, Chang DC (2005) Calcium signaling in apoptosis. Acta Biophys Sin 21:1–18
11. Szalai G, Krishnamurthy R, Hajnoczky G (1999) Apoptosis driven by IP3-linked mitochondrial calcium signals. EMBO J 18:6349–6361
12. Foster KA, Galeffi F, Gerich FJ, Turner DA, Müller M (2006) Optical and pharmacological tools to investigate the role of mitochondria during oxidative stress and neurodegeneration. Prog Neurobiol 79:136–171
13. Wagstaff KM, Dias MM, Alvisi G, Jans DA (2005) Quantitative analysis of protein-protein interactions by native page/fluorimaging. J Fluoresc 15:469–473
14. Li Y, Li M, Xu T (2007) Quantitative time-resolved fluorescence spectrum of the cortical sarcoma and the adjacent normal tissue. J Fluoresc 17:643–648
15. Wang L, Chen T, Qu J, Wei X (2010) Photobleaching-based quantitative analysis of fluorescence resonance energy transfer inside single living cell. J Fluoresc 20:27–35
16. Boisvert S, Joly D, Carpentier R (2006) Quantitative analysis of the experimental O-J-I-P chlorophyll fluorescence induction kinetics apparent activation energy and origin of each kinetic step. FEBS J 273:4770–4777
17. Pittroff W, Dahm F, Blanc F, Keisler D, Cartwright TC (2008) Onset of puberty and the inflection point of the growth curve in sheep-Brody's Law revisited. J Agric Sci 146:239–250
18. van der Heijden GWAM, Vossepoel AM, Polder G (1996) Measuring onion cultivars with image analysis using inflection points. Euphytica 87:19–31
19. Sandau K, Brüne B (1996) The dual role of S-nitrosoglutathione (GSNO) during thymocyte apoptosis. Cell Signal 8:173–177
20. Lin DY, Ma WY, Duan SJ, Zhang Y, Du LY (2006) Real-time imaging of viable-apoptotic switch in GSNO-induced mouse thymocyte apoptosis. Apoptosis 11:1289–1298
21. Bouchier-Hayes L, Muñoz-Pinedo C, Connell S, Green DR (2008) Measuring apoptosis at the single cell level. Methods 44:222–228
22. Johnson LV, Walsh ML, Chen LB (1980) Localization of mitochondria in living cells with Rhodamine 123. Proc Natl Acad Sci USA 77:990–994
23. Martinez AO, Vara C, Castro J (1987) Increased uptake and retention of Rhodamine 123 by mitochondria of old human fibroblasts. Mech Ageing Dev 39:1–9
24. Vannini GL, Pancaldi S, Poli F, Fasulo MP (1988) Rhodamine-123 as a vital stain for mitochondria of plant-cells. Plant Cell Environ 11:123–127
25. Smith JR, Hershkowitz N, Coakley P (1979) Inflection-point method of interpreting emissive probe charateristics. Rev Sci Instrum 50:210–218